Analyst

Accepted Manuscript

ROYAL SOCIETY OF CHEMISTRY

www.rsc.org/analyst

In solution multiplex miRNA detection using DNA-templated silver nanocluster probes

Pratik Shah†[§], Peter Waaben Thulstrup[ϵ§], Seok Keun Cho†, Yong-Joo Bhang[‡], Jong Cheol Ahn[‡], Suk Won Choi[‡], Morten Jannik Bjerrum[ϵ] and Seong Wook Yang†**

†UNIK Center for Synthetic Biology/Plant Biochemistry Laboratory, University of Copenhagen, Thorvaldsensvej 40, DK-1871 Frederiksberg C, Copenhagen, Denmark

[ϵ]Department of Chemistry, University of Copenhagen, Universitetsparken 5, DK-2100, Copenhagen, Denmark

[‡]Seoulin Bioscience Co. Ltd. 4F. #A, KOREA BIO PARK, 700, Daewangpangyo-ro, Bundang-gu, Seongnam-si, Gyeonggi-do, Korea

[§]Equal contributions

*Correspondence E-mail: swyang@life.ku.dk (S.W.Y.) and mobj@chem.ku.dk (M.J.B.)

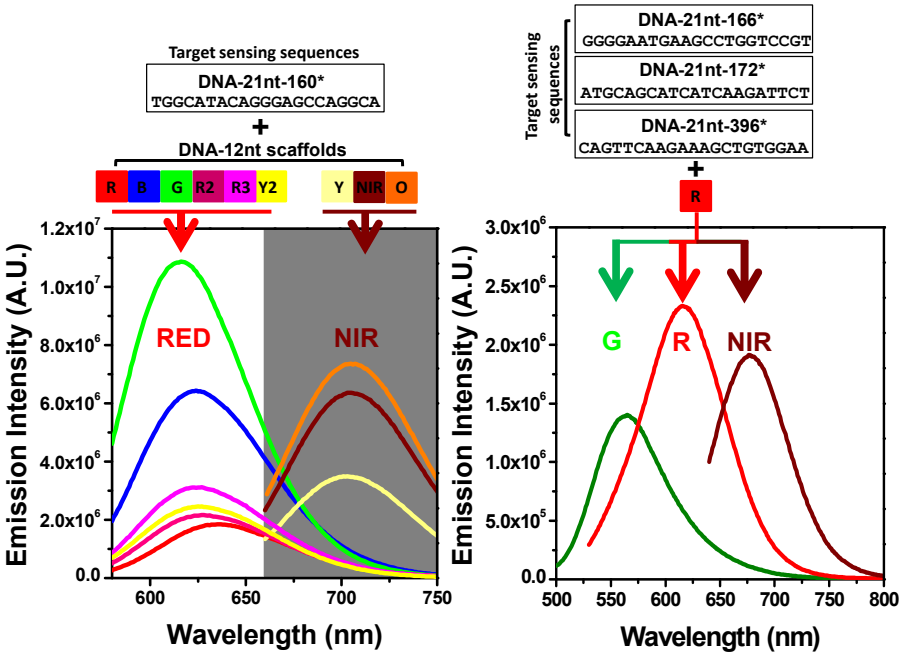

Table of contents entry

ABSTRACT

MicroRNAs (miRNAs) are small regulatory RNAs (size ~21nt to ~25nt) that can be used for biomarkers of disease diagnosis, efforts have been directed towards invention of a rapid, simple and sequence selective detection method for miRNAs. As a case of the efforts, we recently developed a DNA/silver nanoclusters (AgNCs)-based method that light-off in the presence of target miRNA. To further advance our method toward multiplex miRNA detection in solution, designing of varied DNA/AgNCs probes in fluorescence was essential. Therefore, tethering of DNA-12nt scaffolds with 9 different AgNCs emitters to target sensing DNA sequences were investigated. Interestingly, for the creation of spectrally different DNA/AgNCs probes, not only the emitters encapsulated in 9 different DNA-12nt scaffolds were necessary but the tethered target sensing DNA sequences are also crucial to tune the fluorescence across visible to infra-red. In this study, we obtained three spectrally distinctive emitters of each DNA/AgNCs probes such as green, red, and near-infra red fluorescence. Using these DNA/AgNCs probes, we here show a proof of concept for a rapid, one step, and in solution multiplex miRNA detection method.

INTRODUCTION

Due to the attractive optical properties such as brightness, photo-stability and a wide spectral range, the conjugation of silver nanoclusters to DNA sequences has been increasingly used to create nanoscale biosensing systems for selective and specific detection

of biomolecules such as protein[1,2] and nucleic acids. In the case of nucleic acids, the properties of DNA/AgNCs fluorescent have extensively exploited to detect single nucleotide polymorphisms[3-5], specific DNA targets[6,7] and microRNAs[8,9]. The optical properties of DNA/AgNCs are also applied to determine heavy metal ions in water such as copper and mercury[10,11] On the other hand, it has been demonstrated that DNA encapsulated AgNCs can be efficient bio-labels for the microscopic imaging[12-15]. Further, the optical properties of DNA-templated AgNCs are influenced by several parameters – the sequences of DNA templates and their intrinsic secondary structures, the length of DNA templates, reaction buffer, pH, solvent, and oxygen.[16-24] By exploiting the unique spectroscopic features of AgNCs embedded in DNA sequences with tailor-made biological properties, one can achieve rapidly-formed and stable DNA-templated AgNCs (DNA/AgNCs) that can act as sensitive and selective probes. The fluorescence of such a DNA/AgNCs probe, can be monitored either by the induced alteration of the emission intensity and/or by the shift of the emission wavelength in response to the presence of target analytes[1,2,6,7,9-11,16,20,25-31]. We recently demonstrated a method for fast, simple and accurate miRNA detection based on such DNA/AgNCs probe designs[9,30]. As an example of this versatile approach, we produced two DNA/AgNCs probes that target either plant miR160 (involved in phytohormone regulations) or miR172 (important for flower development). The logical next step is development of multiplex target detection methods where for instance a set of tailored probes are capable of detecting a range of different miRNAs. Here, we demonstrate that a set of three DNA/AgNC probes with green, red and near infrared emission allow detection of three individual miRNAs in the same solution, through selective extinction of the probe fluorescence in the presence of complimentary miRNA.

RESULTS AND DISCUSSION

For multiplex miRNA detection using the photoluminescence properties of DNA/AgNCs probes, the design of different miRNA selective probes with spectrally unique features is prerequisite. Richard et al. reported 5 different 12 nucleotide DNA scaffolds (DNA-12nt) with distinctive emission in the red, blue, green, yellow and near-infra red region which we here refer to as DNA-12nt-R, DNA-12nt-B, DNA-12nt-G, DNA-12nt-Y and DNA-12nt-NIR, respectively (see Supporting Information Table 1)[19]. In the recent literature such DNA-12nt scaffolds have been combined with target sensing DNA sequences to construct highly emissive DNA/AgNCs probes[2,3,9,29,32-36] Similarly, Sharma et al. suggested that several DNA templates encapsulating green, orange, red or near-infra red emitters can be created in optimized buffer conditions[16]. On the basis of these studies, we tethered different DNA-12nt scaffolds with 21-nucleotide DNA sequences targeting miR160 (referred as DNA-21nt-160*) to construct 5 different DNA/AgNCs probes (Figure 1A). Surprisingly, when the 5 different DNA-12nt scaffolds were combined with DNA-21nt-160*, each probe only displayed highly emissive fluorescence (λ_{em}=max) of either red or near-infra red color, irrespective of the optical properties of the original DNA-12nt probes (Figure 1B, Table ST1, see Supporting Information Figure 2-9). For instance, when the scaffold giving yellow emission (λ_{em}=~560 nm) was combined with the DNA-21nt-160* sequence, the resulting DNA/AgNCs probe (DNA-12nt-Y-160) showed near-infra red fluorescence (λ_{em} =~710 nm). Similarly, the green emission of DNA-12nt-G (λ_{em}=~525 nm) was altered into red fluorescence (λ_{em} =~625 nm) by tethering to DNA-21nt-160* in the DNA-12nt-G-160 probe (Figure 1).

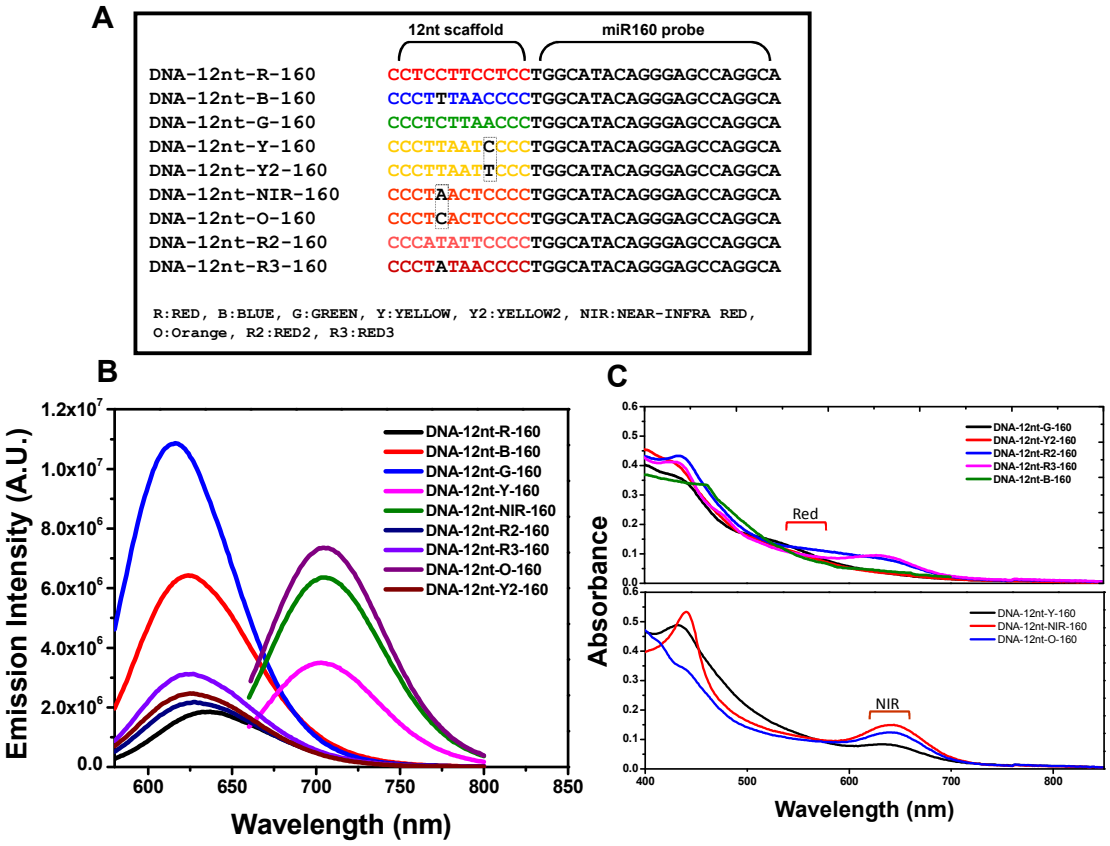

Figure 1: A) DNA sequences of nine DNA/AgNCs probes with their abbreviation used in this study. Each AgNCs creating DNA scaffold is given in its original emissive colors. Single nucleotides substitutions in scaffolds are shown in black. B) Emission spectra of the nine DNA/AgNCs probes. The maximum emission spectra of each DNA/AgNC probes were recorded 1 hour after mixing and reducing the DNA/AgNO3 mixture with NaBH4. C) Absorption spectra of eight DNA/AgNCs probes (15 μM). Top panel shows the absorbance spectra of samples of the probes giving red fluorescence, while the bottom panel shows the same for the NIR emitters. The DNA-12nt-R-160 spectrum has been reported previously[33].

The scaffolds that initially formed red or near-infra red emitters, such as DNA-12nt-R and DNA-12nt-NIR were not notably affected by tethering of the DNA-21nt-160* sequence. The DNA-12nt-B scaffold is known to encapsulate blue emitters (λ_{em} =~480 nm) although we could not observe the blue emission. But by tethering to DNA-21nt-160*, the resulting DNA-12nt-B-160 probe generated red fluorescence (λ_{em} =~625 nm). To further test the fluorescent alterations by the DNA-21nt-160* sequence, we examined 4 additional DNA-12nt scaffolds; DNA-12nt-R2[20], DNA-12nt-R3[20], DNA-12nt-Y2, and DNA-12nt-O (see Supporting Information Table 1). Notably, the tethering of each of these four extra scaffolds to DNA-21nt-160* also resulted in either red (λ_{em} =~625 nm) or near-infra red (λ_{em} =~710 nm) emissive species (Figure 1B). The scaffolds DNA-12nt-R2 and DNA-12nt-R3 emitted slightly different red fluorescence with maxima of 655 nm and 640 nm, respectively. By the attachment of DNA-21nt-160*, these two scaffolds generated a synchronized red fluorescence at 620 nm. Another yellow emitter, DNA-12nt-Y2 (λ_{em} =~580 nm) has a C→T nucleotide substitution at 9th cytosine of DNA-12nt-Y, and this altered emission to red color (λ_{em} =~625 nm) when coupled with DNA-21nt-160*. Finally, the clear orange fluorescence of DNA-12nt-O scaffold which has single nucleotide difference to DNA-12nt-NIR was dramatically changed to the near-infra red (λ_{em} =~710 nm) when tethered to the DNA-21nt-160* sequence. To sum up, we systematically reproduced the distinctive fluorescence patterns of a series of previously reported 12nt scaffolds (except for DNA-12nt-B) as we show in Supporting Information Figure 1. But under our experimental conditions, all the tested DNA-12nt scaffolds changed emission properties when coupled with the DNA-21nt-160* sequence, forming red or infrared emitting species only. The emission spectra of the new series of red/infrared emitters are shown in Figure 1B. The corresponding absorbance spectra (Figure 1C) show that most species have main long-wavelength absorbance peaks that

coincide with the excitation wavelength producing the highest emission, yet all samples do have multiple, broad bands in the visible region. Full Ex/Em spectral scans of all the DNA/AgNCs probes can be seen in Supporting Information figures 2 to 9, showing a unique pattern of spectra for each probe. These findings bring new light to how subtle sequence variations determine the type of emitters that are encapsulated in the DNA, although the 3-dimensional structures of the formed/AgNCs probes are not explicitly known. For instance, as stated above, a single nucleotide substitution in the DNA-12nt-Y scaffold of DNA-12nt-Y-160 probe led the emission shifting from 710 nm to 620 nm, (see Supporting Information Figure 4A). On the contrary, the DNA-12nt-B sequence (5th thymine, reported as blue) has a single nucleotide exchanged compared to DNA-12nt-R3 (5th adenine, red) and both generated red fluorescence at 540 nm excitation by tethering DNA-21nt-160* (Supporting Information Figure 2B). Also, by attachment of DNA-21nt-160*, the emission of DNA-12nt-O (5th cytosine, orange) and DNA-12nt-NIR (5th Adenine, near-infra red) converged toward the near-infra red fluorescence of 710 nm (see Supporting Information Figure 7B). These results strongly suggest that the base sequences of the DNA-12nt scaffold is not the decisive factor for the obtained spectral properties of the combined probes. Previous studies mainly discuss two parameters; namely the base sequence and length of the DNA scaffolds, but in this context it is hard to explain the presently observed convergence of the numerous emitters into red or near-infra red emitting species. Therefore, we here carefully infer the involvement of another factor, namely secondary structure of the DNA/AgNCs probes in the determination of emitter types. This is in line with our previous report showing that the secondary structures of DNA/AgNCs probes are important for the rapid formation of highly emissive red AgNCs species[30]. We proceeded to apply gel electrophoresis and high resolution melting (HRM) analysis to investigate the structure formation of nine DNA/AgNCs probes with the DNA-

21nt-160* sequence attached. The resulting data shows that all the tested DNA/AgNC probes with nine different scaffolds display up-shifted bands that indicate the presence of secondary structures such as mismatch self-dimer or hair-pin structures (see Supporting Information Figure 11). Furthermore, all the DNA/AgNCs probes have much higher Tm values than single strands, confirming the presence of secondary structures in the DNA/AgNCs probes (see Supporting Information Figure 12). These results on longer sequences thus support the involvement of specific nucleic acid secondary structure in the rapid formation of the DNA/AgNCs probes with red or near-infra red fluorescence, independently of the original colors of the DNA-12nt scaffolds. With this knowledge, the next step towards multiplex detection was to investigate the effect of different target sensing DNA sequences on the fluorescence shifts. For the design of scaffolds, we selected DNA-12nt-R combined with three target sensing DNA sequences, namely DNA-21nt-172*, DNA-21nt-166*, and DNA-21nt-396*, that target miR172, miR166, and miR396, respectively. As shown in Figure 2A, we denoted these DNA/AgNCs probes as DNA-GG172-12nt-RED, DNA-12nt-RED-166 and DNA-12nt-RED-396. First, we examined the full spectral scans of the DNA/AgNCs probes (1.5 μM, 1h incubation) to observe the influence of target sensing DNA sequences on their spectral characteristics (see Supporting Information 13). For these three probes, the highest emission (~620 nm) of the DNA-12nt-R scaffold was differentiated when combined with the different DNA complementary sequences: DNA-GG172-12nt-RED shows a maximum fluorescence at 620 nm when excited at 540 nm whereas DNA-12nt-RED-166 peaks at 680 nm with excitation at 620 nm. DNA-12nt-RED-396 shows a maximum fluorescence at 560 nm when excited at 480 nm, this being by far most distinctive green color, one that is not obtained from any of the other DNA/AgNCs probes (Figure 2B).

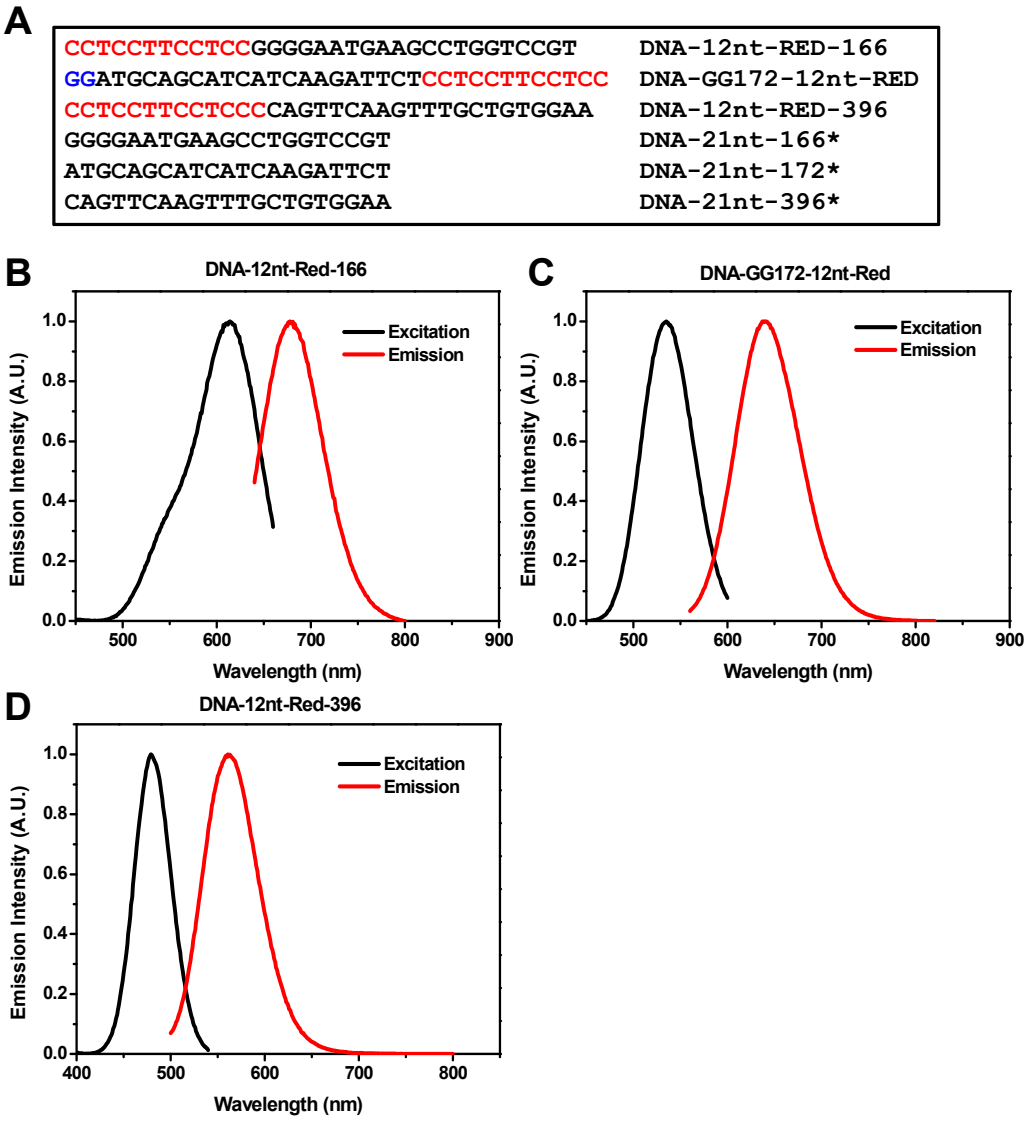

Figure 2: A) DNA sequences of DNA-12nt-RED-166, DNA-GG172-12nt-RED, and DNA-12nt-RED-396 probes. The target complementary sequences of each DNA/AgNCs probes are designated as DNA-21nt-166*, DNA-21nt-172*, and DNA-21nt-396*. In red, the original red emissive AgNC creating part (DNA-12nt-RED) is given. Extra sequences for the secondary structure formation of DNA-GG172-12nt-RED are given as blue. B) Excitation and emission spectra of the DNA-12nt-RED-166 probe. The emission spectra (excited at 620 nm) were recorded 1h after mixing and reducing with $AgNO_3$ and $NaBH_4$. The excitation spectrum

(monitored at 680 nm) was recorded following the same AgNCs creation procedure. C) Excitation and emission spectra of the DNA-GG172-12nt-RED probe. The emission spectra (excited at 540 nm) were recorded 1h after mixing and reducing with $AgNO_3$ and $NaBH_4$. The excitation spectrum (monitored at 620 nm) was recorded following the same AgNCs creation procedure. D) Excitation and emission spectra of the DNA-12nt-RED-396 probe. The emission spectra (excited at 480 nm) were recorded 1h after mixing and reducing with $AgNO_3$ and $NaBH_4$. The excitation spectrum (monitored at 560 nm) was recorded following the same AgNCs creation procedure.

While DNA-12nt-RED-166 showed dispersed peaks from red to near-infra red upon 20 nm shifts of the excitation wavelength from 520 nm to 680 nm, DNA-GG172-12nt-RED and DNA-12nt-RED-396 displayed highly aligned emissions at 620 nm and 560 nm, respectively (see Supporting Information Figure 13). Although these three DNA/AgNCs probes harbour the original DNA-12nt-R scaffold, the assembled probes with three different target sensing sequences emit highly distinctive patterns of fluorescence. Moreover, as shown in Supporting Information Figure 14, the 21 nucleotide target sensing DNA sequences alone (1.5 μM, 1h incubation) are unable to form any emissive AgNCs species without attachment of the DNA-12nt-R scaffold, also implying the pivotal role of what is likely a structural factor beyond the base sequences of DNA-12nt-R and target sensing DNA fragments. Taken all together, the results so far clearly indicate that the sequence of the DNA-12nt scaffolds is not the only determinant of the spectral characteristics of DNA/AgNCs. The indication can also be deduced from Yeh et al.'s research showing how a strong red fluorescence can be generated from a DNA target sensing sequences with a yellow scaffold[7]. As shown in Figure 2 the

spectral characteristics of the three designed DNA/AgNCs probes - DNA-GG172-12nt-RED ($\lambda_{ex}/\lambda_{em}$ =540/620 or 500/620 nm), DNA-12nt-RED-166 ($\lambda_{ex}/\lambda_{em}$ =620/680 nm), and DNA-12nt-RED-396 ($\lambda_{ex}/\lambda_{em}$ =480/560 nm) are differentiated to a degree to potentially allow for in-solution multiplex miRNA detection. However, to establish an in-solution multiplex detection method, a number of essential conditions are prerequisite. First, the target specificity of each DNA/AgNCs probe needs to be established under high stringency conditions and furthermore, the optimal buffer composition needs to be determined. Extensive testing for determination of the optimal buffer conditions was undertaken (details not shown), where both the overall fluorescence yield of the probes and the extinction ratio (I_0/I) in the presence of target RNA was taken into account. Subsequently under the obtained optimized buffer conditions (2mM Tris-acetate), we tested the target specificity of the DNA/AgNCs probes against non-specific miRNAs. The DNA-GG172-12nt-RED probe was incubated with several non-target miRNAs such as RNA-miR160, RNA-miR166, RNA-miR396, RNA-miR869, and human RNA-miR-21 (Figure 3A). Similar to the results in our previous report[30], the DNA-GG172-12nt-RED probe successfully distinguished its specific target RNA-miR172 from non-specific targets, also in the new buffer system. As shown in the inset of Figure 3C, the DNA-GG172-12nt-RED probe displays I_0/I value of 7 when it encounters RNA-miR172. It is also notable that the strong red emission of the DNA-GG172-12nt-RED probe was hardly diminished in the presence of the non-specific miRNAs. This clearly proves that the DNA-GG172-12nt-RED probe is able to specifically detect its target, RNA-miR172. Likewise, the two newly designed probes, DNA-12nt-RED-166 and DNA-12nt-RED-396 also successfully distinguished their own targets (Figure 3B, 3D). The highest extinction ratios (I_0/I) were observed by addition of specific targets, RNA-miR166 or RNA-miR396, in contrast to the marginal effects of non-specific targets (Figure 3B, 3D, inset).

Intriguingly, we noted that RNA-miR396 and RNA-miR869 rather elevated the emission of the DNA-GG172-12nt-RED probe about 2-fold and 1.5-fold, respectively (Figure 3C). Generally, many of the tested non-specific targets slightly increased the emission intensity of the DNA-12nt-RED-166 probe (Figure 3B) and the DNA-12nt-RED-396 (Figure 3D). Currently, we speculate that the elevated emission may be due to further stabilization of structures (triplex or otherwise) by partial or non-specific base paring between the structured probes and targets where additional emissive AgNCs can be encapsulated[37].

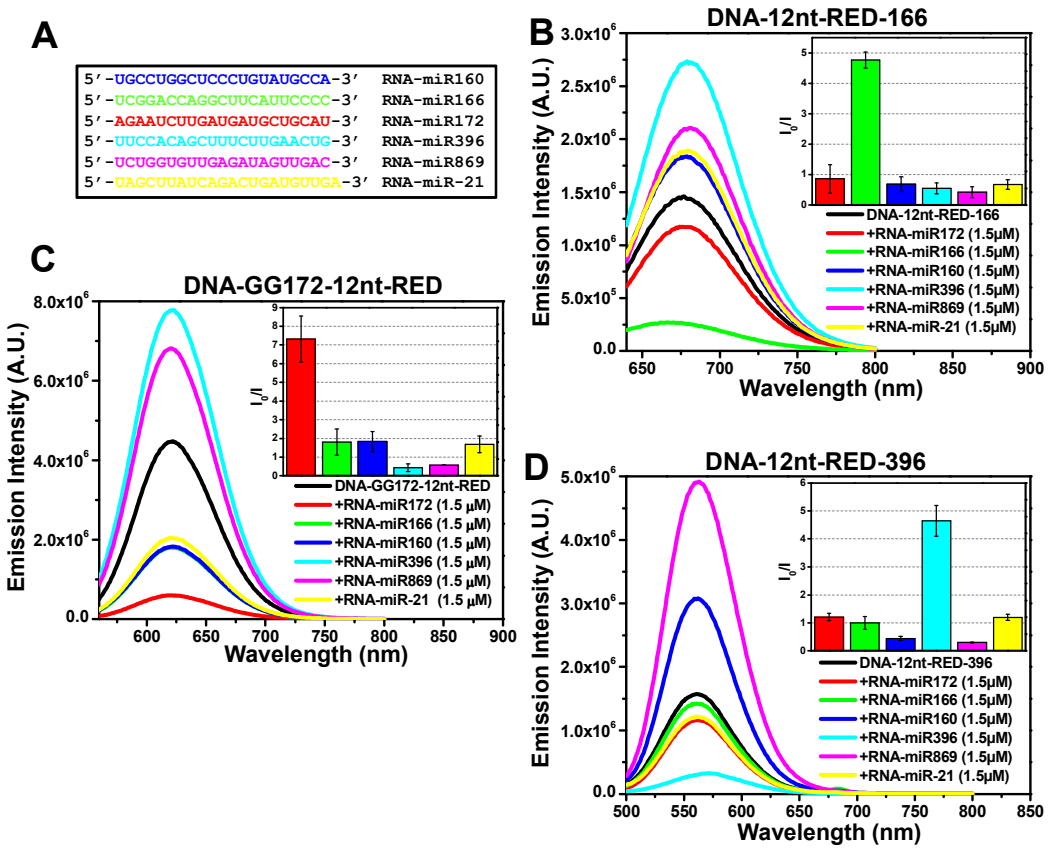

Figure 3: A) Target miRNA sequences used in this study. For the DNA probes, the original red emissive AgNC creating part (DNA-12nt-RED) is shown colored in red, complementary sequences to miRNA targets are shown in black, and additional sequences included for structure formation in the DNA-GG172-12nt-RED probe are shown in blue. B) Specificity

assessment of the DNA-12nt-RED-166 probe towards different miRNAs measured as the emission spectra obtained following excitation at 620 nm. 1.5 μM DNA-12nt-RED-166 probe (black trace). Mixture of 1.5 μM DNA-12nt-RED-166 probe with 1.5 μM of RNA-miR160 (blue trace), RNA-miR166 (green trace), RNA-miR172 target (red trace), RNA-miR396 (sky-blue trace), RNA-miR869 (pink trace), and RNA-miR-21 (yellow trace). Insert shows the corresponding I_0/I values. C) Specificity assessment of the DNA-GG172-12nt-RED probe to the same set of miRNAs as shown in panel B. Inset shows I_0/I values. The average of 3 repeats used for data. D) Specificity assessment of the DNA-12nt-RED-396 probe to the same set of miRNAs as shown in panel B. Inset shows I_0/I values. The average of 3 repeats is presented.

The elevated red fluorescence emission from RNA-miRNA/AgNCs can be excluded although ribonucleic acids are known to be able to encapsulate emissive AgNC[38] (Supporting Information Figure 15). The emission elevation upon binding of non-specific targets in our method may actually prove to be an advantage in discriminating a target on *in vivo* samples, due to the background presence of non-specific endogenous RNAs, where multiple non-specific hybridization reactions can proceed simultaneously. We speculate that the increased emission may be caused by structures formed that override the thermodynamic penalty of mismatches between non-specific target and DNA probe that may accommodate additional emissive AgNCs. The emission drop of DNA probes upon recognition is most likely caused only by the perfect Watson–Crick hybridization between a DNA probe and its complementary target. However, to confirm this, a detailed study using near-perfect single mismatch targets must be performed. In the present study, the target specificity of DNA/AgNCs probes was sufficient to proceed to in-solution multiplex miRNA detection. For multiplex detection, the interference amongst the different probes needs to be investigated. To test the emission

interferences, equal amounts of each DNA/AgNCs probe (1.5 μM) was mixed in a reaction solution and the fluorescence pattern of the mixed solution was observed using the same method as previously described. The maximum emission of DNA-12nt-RED-396 and DNA-12nt-RED-166 were not altered in the mixed solution, while the strong red fluorescence of DNA-GG172-12nt-RED was mostly overlapped with the red emission of DNA-12nt-RED-166 when excited at 540 nm (see Supporting Information 16A). To avoid the interference of emissions between DNA-GG172-12nt-RED and DNA-12nt-RED-166, we took advantage of the highly aligned emission profile of DNA-GG172-12nt-RED that generates only the red fluorescence at ~620 nm through excitation from 480 nm to 580 nm. We excited at 510 nm instead 540 nm, by which the strong red fluorescence of DNA-12nt-RED-166 became quiescent where DNA-GG172-12nt-RED was still highly emissive (see Supporting Information Figure 16). Through this excitation adjustment, we obtained three distinctive emission colors in a solution with three DNA/AgNCs probes without interferences as shown in Figure 4A. The high target selectivity of DNA/AgNCs probes is critical to the reliability of in-solution multiplex analysis. To examine the target selectivity of the three DNA/AgNCs probes in solution, we performed a target selectivity assay by adding each target miRNA at a time to the mixture of three probes. As shown above, without target miRNAs, the three distinctive emissions in the mixture of three DNA/AgNCs probes were clearly observed (Figure 4A). Upon addition of RNA-miR166 (1.5 μM) to the solution of three DNA/AgNCs probes, only the near-infra red emission at ~620 nm excitation which originates from DNA-12nt-RED-166 was significantly diminished without hindering the green and near-infra red emissions (Figure 4B). Addition of RNA-miR172 (1.5 μM) to a solution that dropped only red emission at 540 nm excitation which originates from DNA-GG172-12nt-RED (Figure 4C). Likewise, the green emission at 480 nm excitation was specifically diminished by

addition of RNA-miR396 (1.5 μM) (Figure 4D). These data clearly confirmed that in-solution multiplex miRNA detection using the varied fluorescent DNA/AgNCs probes is technically possible. Moreover, we also tested the combination of two miRNA targets at the same time. Simultaneous addition of RNA-miR172 and RNA-miR166 reduced both the red and near-infra red fluorescence and the green emission is intact (Figure 4E). Also, addition of RNA-miR172 and RNA-miR396 to the mixture of the three DNA/AgNCs probes resulted only in strong near-infra red fluorescence from DNA-12nt-RED-166 (Figure 4F). Along the same line, the addition of two miRNAs, RNA-miR166 and RNA-miR396, specifically extinguished the near-infrared (corresponds to RNA-miR166) and green (corresponds to RNA-miR396) fluorescence (Figure 4G).

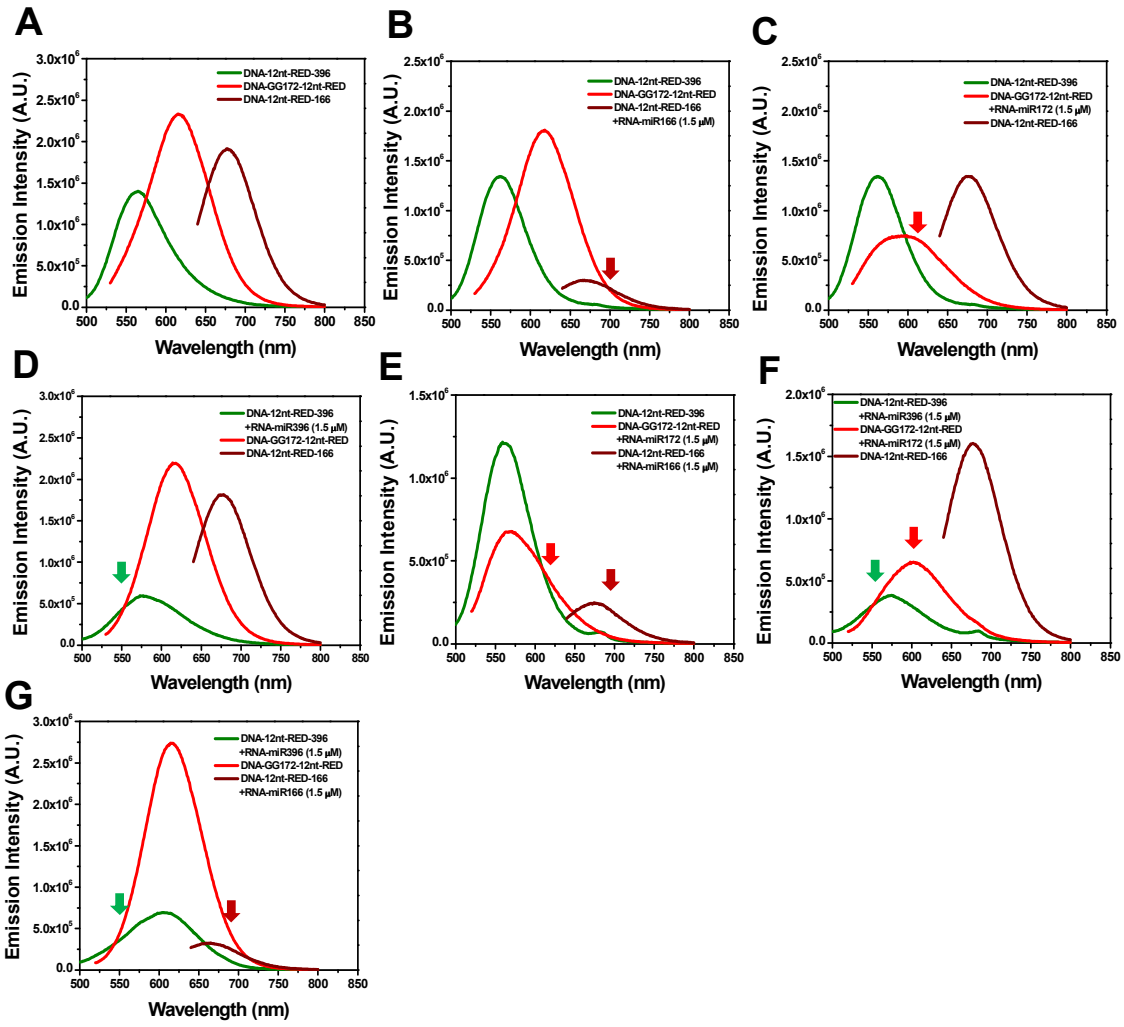

Figure 4: A) Emission spectra of three DNA/AgNCs probes in a reaction solution, DNA-12nt-RED-396 (green curve, λex/em=480/560 nm), DNA-GG172-12nt-RED (red curve, λex/em=540/620 nm), and DNA-12nt-RED-166 (wine curve, λex/em=620/680 nm). B) Specific emission drop of DNA-12nt-RED-166 (1.5 μM) by addition of RNA-miR166 (1.5 μM). C) Specific emission drop of DNA-GG172-12nt-RED (1.5 μM) by addition of RNA-miR172 (1.5 μM). D) Specific emission drop of DNA-12nt-RED-396 (1.5 μM) by addition of RNA-miR396 (1.5 μM). Colored arrow heads indicate the position of emission drops. E) Emission drops of DNA-12nt-RED-166 (1.5 μM) and DNA-GG172-12nt-RED (1.5 μM) by addition of RNA-miR166 (1.5 μM) and RNA-miR172 (1.5 μM). F) Emission drops of DNA-GG172-12nt-RED (1.5 μM) and DNA-12nt-RED-396 (1.5 μM) and by addition of

RNA-miR172 (1.5 μM) and RNA-miR396 (1.5 μM). G) Emission drops of DNA-12nt-RED-166 (1.5 μM) and DNA-12nt-RED-396 (1.5 μM) and by addition of RNA-miR166 (1.5 μM) and RNA-miR396 (1.5 μM).

To corroborate the specificity of our in solution-method, a series of capillary electrophoresis experiments were performed to establish whether or not the DNA/AgNCs probes interact with each other in the absence and presence of target miRNA. In Figure 5 A and B the individual capillary electrophoresis traces of DNA-12nt-RED-166 and DNA-GG172-12nt-RED are shown. These two probes have similar retention times, but as Figure 5 C and D clearly illustrate, they do not interact in solution. To investigate the specificity of miRNA hybridization under the same conditions, the experiment was repeated (Figure 5E) this time by adding RNA-miR166 (Figure 5F) or RNA-miR172 (Figure 5G). These capillary electrophoresis results also clearly show that the retention peak of each probe is specifically shifted by its target miRNA addition. Taken together, the results shown in Figures 4 and 5 demonstrate that the individual fluorescence of three DNA/AgNCs probes can be selectively extinguished, and that they interact exclusively with the target miRNA in the solution. These findings provide evidence for both high target selectivity and the non-interference of the other components of the complex mixtures of probes and targets. This holds great promise for the further practical application of this novel multiplex miRNA detection method.

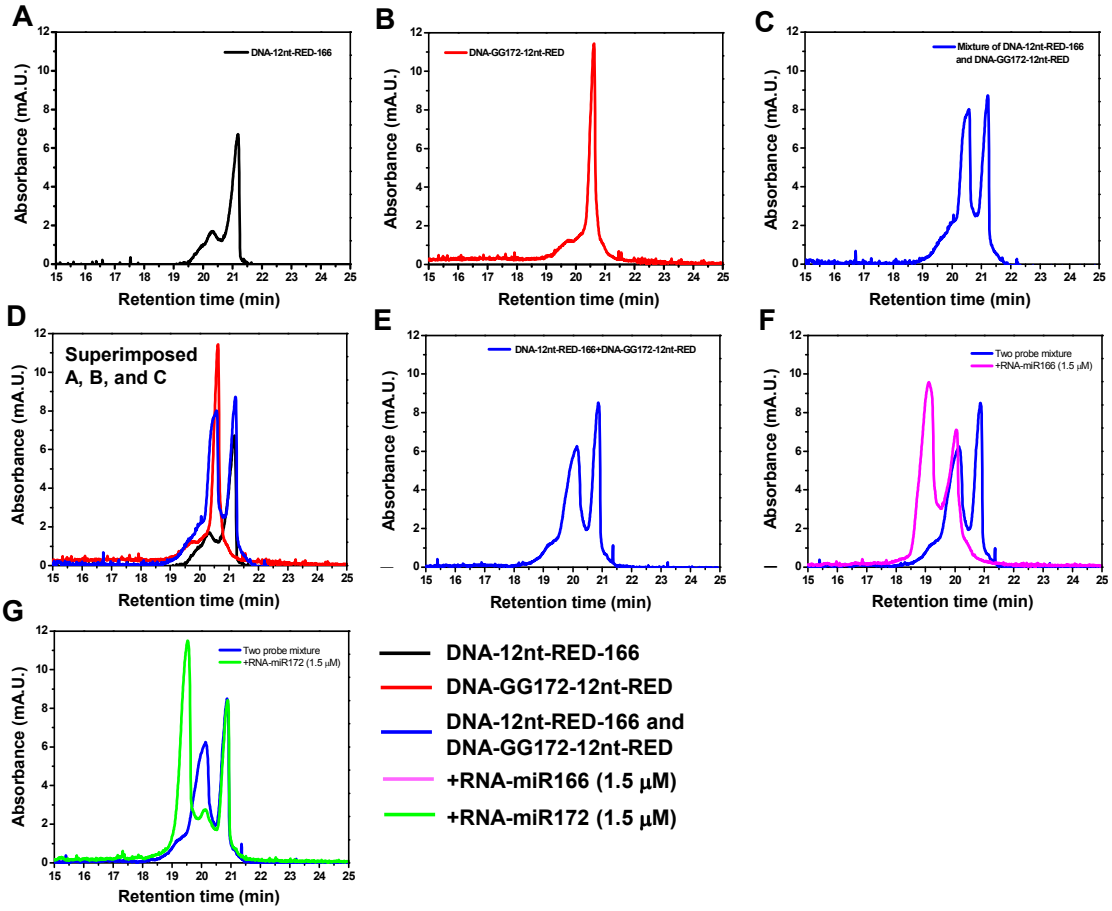

Figure 5: Electropherograms by capillary electrophoresis showing separation as function of time of DNA/AgNCs probes. Separating conditions see supporting information. A) Retention peak of DNA-12nt-RED-166. B) Retention peak of DNA-GG712-12nt-RED. C) Retention peaks of DNA-12nt-RED-166 and DNA-GG172-12nt-RED which are mixed in a reaction solution. D) Superimposed peaks from A), B) and C) shows non-interference of two probes in solution. E) Control showing the non-interfered retention peaks of DNA-12nt-RED-166 and DNA-GG172-12nt-RED. F) Addition of RNA-miR166 specifically induces the peak shift of DNA-12nt-RED-166. G) Addition of RNA-miR172 specifically induces the peak shift of DNA-GG172-12nt-RED.

EXPERIMENTAL

Materials and Reagents. DNA probes and desalted miRNA targets were obtained from three different commercial suppliers: IDT (Integrated DNA Technologies, BVBA. Interleuvenlaan 12A, 3001 Leuven, Belgium). The synthesis of emissive AgNCs was carried out using $AgNO_3$ (99.9999%) and $NaBH_4$ (99.99%) from Sigma Aldrich. Tris-Acetate buffer (pH 7, 0.5 M) was prepared with TRIZMA® acetate salt (≥99.0%, from Sigma Aldrich) in pure Milli-Q water (18.2MΩ.cm).

Synthesis of DNA/AgNCs probes and target miRNA detection.

Fluorescent AgNCs probes were made by individually incubate the nine DNA/AgNCs probes. DNA-GG172-12nt-RED, DNA-12nt-RED-396, and the DNA-12nt-RED-166 (15 μM) probes were incubated at 25ºC for 1 min in the given concentrations of Tris-acetate buffer with or without salts, followed by an addition of $AgNO_3$ (250 μM) and $NaBH_4$ (250 μM), (1:17:17) to a final volume (50 μl). For the miRNA detection assay, we added a fixed amount of various targets (15 μM); RNA-miR160, RNA-miR166, RNA-miR172, RNA-miR396, RNA-miR869 and RNA-miR-21 to the DNA-GG172-12nt-RED, DNA-12nt-RED-396 or DNA-12nt-RED-166 (15 μM) at the given concentrations of Tris-acetate buffer and incubated for 15 min at 25ºC. Then, $AgNO_3$ (250 μM) and $NaBH_4$ (250 μM) were added to the RNA/DNA mixtures to a final volume (50 μl). All the DNA/AgNCs were incubated for 1h at 25ºC and diluted with 450 μl of distilled water before measurement on a fluorimeter (Horiba Jobin Yvon, Fluoromax-4) in a 10 mm disposable cuvette. We here designated the concentrations of nucleic acids and buffer in the final volume for measurements (500 μl).

Emissive DNA/AgNC using DNA-12nt scaffold as mentioned in Table 1 were prepared following similar method as published[19,20]. To make fluorescent AgNCs using DNA-12nt-Scaffold, the 15μM of DNA probes were mixed with AgNO3 (90 μM) and NaBH4 (90 μM) (1:6:6) under the similar buffer conditions as reported. The reaction mixtures were incubated at 4°C for 24 hours before measuring fluorescence emission. Absorbance measurements were performed on undiluted samples using a Shimadzu UV 2401PC instrument using a 10 mm Hellma quartz cuvette with 1 nm bandwidth setting and medium scan speed.

Multiplex miRNA Detection assay:

For the multiplex miRNA detection assay presented in Figure 4, each probe (DNA-GG172-12nt-RED, DNA-12nt-RED-166 and DNA-12nt-Red-396) was mixed with equimolar concentration (15μM each) in a 1.5 ml eppendorf tube with or without target microRNA (10 μM) each. The reaction mixture was then mixed with Tris-acetate buffer. The DNA/RNA mixture in the presence of Tris-acetate buffer were denatured at 100°C for 10 min and immediately transferred to 25°C to facilitate annealing between DNA/RNA. Then, to make fluorescent AgNCs, the DNA probes were mixed with AgNO3 (250 μM) and NaBH4 (250 μM) (1:17:17) to a final volume (125 μL). For all the fluorescence excitation and emission spectra recorded for the above mentioned experiments, the samples were diluted with 375 μL (the final concentration of each DNA probes is 1.5 μM) of Milli-Q water and measurements were performed with a fluorimeter (Horiba Jobin Yvon, Fluoromax-4) in 10 mm plastic disposable cuvettes.

Non-denaturing Polyacrylamide Gel Electrophoresis:

To detect the mismatch self-dimer structures from the DNA/AgNC compounds, gel electrophoresis analysis was performed with a native polyacrylamide gel (20%). A Mini-PROTEAN Tetra Cell system (Bio-Rad) was used for the gel electrophoresis with a TBE buffer (Tris base; 44.5 mM, Boric acid; 44.5 mM, EDTA; 1mM). Gel electrophoresis experiments were performed starting from 45 μM solutions of DNA/AgNC mixed with GelPilot DNA loading dye 5X (Qiagen) before loading on to Gel. The gel was run for 6 hours at 60V in ice. The native gel was imaged on G-Box from Syngene using Genesnap software (Syngene).

High Resolution Melting:

High-resolution melting analysis was performed with a Rotergene Q (Qiagene). For this, 45 μM of the DNA probes was mixed with 10 μM SYBR Green I 10,000X (Invitrogen) in a final volume of 15 μL. The temperature was increased from 25°C to 98°C, at a rate of 1°C per 4 s, and the emission was monitored at 510 nm. Native DNA without AgNCs was used in the HMR experiments and the observed green emission (monitored at 510nm) is from the added SYBR green dye.

Capillary electrophoresis:

Capillary electrophoresis (CE), is a technique widely used for separation of biomolecules. Separated compounds appear as peaks with different retention times in an electropherogram. The method is a useful tool in the analysis of binding affinities between DNA/AgNC probes.

The experiments were performed with a Hewlett Packard 3D Capillary Electrophoresis apparatus with an internal diode array Uv-vis spectrofotometer as detector. A silica capillary (64.5 cm x 50 μm i.d.) with 56.0 cm to the detection window was used. The capillary was in every run flushed with 0.1 M NaOH for two minutes, followed by wash with buffer for another two minutes. Samples were applied for 10 s at a pressure of 50 mbar and the run was started with positive to negative potential. All experiments were performed at 20 kV and 15 ^{o}C. Buffer was in all runs 20 mM Tris-Acetate, pH = 6.5. The buffers in the inlet and outlet reservoirs were changed after each run to avoid pH changes. All CE experiments were performed at least twice.

CONCLUSION

In summary, the presented results have shown that reliable specificity coupled with a unique spectroscopic response upon target miRNA hybridization in a more complex situation, a multi-chromatic detection scheme, can be established. Although a recent study showed that the creation of DNA sensors emitting two different colours for dual miRNA detection is possible by tethering the two different DNA scaffolds[8], we suggested here that the strategy, exploiting of various colours from various DNA scaffolds, is not easily accomplished due to the unknown features of emissive AgNCs formation. Furthermore, our method has several strengths in addition to its simplicity and facility of use: 1) while it is comparable to conventional small RNA blot analysis, the target sensitivity of our method is not higher than amplification-based methods. However, it is a strong point that the direct detection of the endogenous levels of miRNA, will lead to fewer false positive signals. 2) Our method does not require any immobilization, modification, amplification, and signal enhancement in which time-consuming chemical reactions, additional enzymes, and processing steps are

necessary. 3) Multiple miRNA targets, here monitored at three different wavelengths, can be detected in a complex solution.

Through this study, we observed two intriguing spectral phenomena. First, the systematic fluorescence shifting of DNA-12nt scaffolds by tethering of target sensing DNA sequences. Second, the surprising emission enhancement of a given DNA/AgNCs probe upon hybridization of non-specific miRNAs. Also, we can conclude that the application of various DNA-12nt scaffolds with distinctive spectral features is not *per se* a route to the rational design of a selection of multichromatic DNA/AgNCs probes. This clearly implies that the DNA-12nt scaffold alone is not responsible for the encapsulation of highly emissive silver nano-clusters, but that the structure and conformation of the entire nucleic acid polymer must be considered. However, knowledge on the exact molecular mechanisms and structures that lead to the appearance of highly fluorescent DNA/AgNCs probes is still limited. For further insight into the fascinating phenomena of highly emissive DNA/AgNCs probes detailed knowledge on the rules underlying spectral determinants have to be established, and can in turn lead the rational design of a new generation of analytical nano-technological probes.

ASSOCIATED CONTENTS

Procedure details for the creation of emissive AgNCs and buffer optimization. Full scan spectra of nine DNA/AgNCs probes, DNA-12nt-RED-166, DNA-GG172-12nt-RED, and DNA-12nt-RED-396 in Tris-acetate buffer. Full spectra scan of target complementary DNA sequences, miR396 and miR869. HRM analysis and gel electrophoresis analysis of nine DNA/AgNCs probes.

ACKNOWLEDGMENT

S.W.Y. gratefully acknowledges financial support from the "Centre for Synthetic Biology" at Copenhagen University funded by the UNIK research initiative of the Danish Ministry of Science, Technology and Innovation (Grant 09-065274). We appreciate Thomas Günter-Promosky for use of his fluorimeter which is supported by Carlsbergfondet.

REFERENCES

(1) Liu, X.; Wang, F.; Niazov-Elkan, A.; Guo, W.; Willner, I. *Nano Lett* **2013**, *13*, 309.
(2) Sharma, J.; Yeh, H. C.; Yoo, H.; Werner, J. H.; Martinez, J. S. *Chem Commun (Camb)* **2011**, *47*, 2294.
(3) Park, J.; Lee, J.; Ban, C.; Kim, W. J. *Biosens Bioelectron* **2013**, *43*, 419.
(4) Yeh, H. C.; Sharma, J.; Shih Ie, M.; Vu, D. M.; Martinez, J. S.; Werner, J. H. *J Am Chem Soc* **2012**, *134*, 11550.
(5) Guo, W.; Yuan, J.; Dong, Q.; Wang, E. *J Am Chem Soc* **2010**, *132*, 932.
(6) Liu, X.; Wang, F.; Aizen, R.; Yehezkeli, O.; Willner, I. *J Am Chem Soc* **2013**, *135*, 11832.
(7) Yeh, H. C.; Sharma, J.; Han, J. J.; Martinez, J. S.; Werner, J. H. *Nano Lett* **2010**, *10*, 3106.
(8) Zhang, M.; Liu, Y. Q.; Yu, C. Y.; Yin, B. C.; Ye, B. C. *Analyst* **2013**, *138*, 4812.
(9) Yang, S. W.; Vosch, T. *Anal Chem* **2011**, *83*, 6935.
(10) Su, Y. T.; Lan, G. Y.; Chen, W. Y.; Chang, H. T. *Anal Chem* **2010**, *82*, 8566.
(11) Guo, W.; Yuan, J.; Wang, E. *Chem Commun (Camb)* **2009**, 3395.
(12) Antoku, Y.; Hotta, J.; Mizuno, H.; Dickson, R. M.; Hofkens, J.; Vosch, T. *Photochem Photobiol Sci* **2010**, *9*, 716.
(13) Yu, J.; Choi, S.; Dickson, R. M. *Angew Chem Int Ed Engl* **2009**, *48*, 318.
(14) Yu, J.; Choi, S.; Richards, C. I.; Antoku, Y.; Dickson, R. M. *Photochem Photobiol* **2008**, *84*, 1435.
(15) Vosch, T.; Antoku, Y.; Hsiang, J. C.; Richards, C. I.; Gonzalez, J. I.; Dickson, R. M. *Proc Natl Acad Sci U S A* **2007**, *104*, 12616.
(16) Sharma, J.; Yeh, H. C.; Yoo, H.; Werner, J. H.; Martinez, J. S. *Chem Commun (Camb)* **2010**, *46*, 3280.
(17) Sengupta, B.; Springer, K.; Buckman, J. G.; Story, S. P.; Abe, O. H.; Hasan, Z. W.; Prudowsky, Z. D.; Rudisill, S. E.; Degtyareva, N. N.; Petty, J. T. *J Phys Chem C* **2009**, *113*, 19518.
(18) O'Neill, P. R.; Velazquez, L. R.; Dunn, D. G.; Gwinn, E. G.; Fygenson, D. K. *J Phys Chem C* **2009**, *113*, 4229.

(19) Richards, C. I.; Choi, S.; Hsiang, J.-C.; Antoku, Y.; Vosch, T.; Bongiorno, A.; Tzeng, Y.-L.; Dickson, R. M. *J Am Chem Soc* **2008**, *130*, 5038.
(20) Patel, S. A.; Richards, C. I.; Hsiang, J. C.; Dickson, R. M. *J Am Chem Soc* **2008**, *130*, 11602.
(21) Gwinn, E. G.; O'Neill, P.; Guerrero, A. J.; Bouwmeester, D.; Fygenson, D. K. *Adv Mater* **2008**, *20*, 279.
(22) Ritchie, C. M.; Johnsen, K. R.; Kiser, J. R.; Antoku, Y.; Dickson, R. M.; Petty, J. T. *J Phys Chem C Nanomater Interfaces* **2007**, *111*, 175.
(23) Petty, J. T.; Zheng, J.; Hud, N. V.; Dickson, R. M. *J Am Chem Soc* **2004**, *126*, 5207.
(24) Shah, P.; Cho, S. K.; Thulstrup, P. W.; Bhang, Y. J.; Ahn, J. C.; Choi, S. W.; Rorvig-Lund, A.; Yang, S. W. *Nanotechnology* **2014**, *25*, 045101.
(25) Petty, J. T.; Fan, C.; Story, S. P.; Sengupta, B.; Iyer, A. S.; Prudowsky, Z.; Dickson, R. M. *J Phys Chem Lett* **2010**, *1*, 2524.
(26) Li, W.; Hu, Y.; Xia, Y.; Shen, Q.; Nie, Z.; Huang, Y.; Yao, S. *Biosens Bioelectron* **2013**, *47*, 345.
(27) Petty, J. T.; Story, S. P.; Juarez, S.; Votto, S. S.; Herbst, A. G.; Degtyareva, N. N.; Sengupta, B. *Anal Chem* **2012**, *84*, 356.
(28) Liu, X.; Zong, C.; Lu, L. *Analyst* **2012**, *137*, 2406.
(29) Han, S.; Zhu, S.; Liu, Z.; Hu, L.; Parveen, S.; Xu, G. *Biosens Bioelectron* **2012**, *36*, 267.
(30) Shah, P.; Rorvig-Lund, A.; Chaabane, S. B.; Thulstrup, P. W.; Kjaergaard, H. G.; Fron, E.; Hofkens, J.; Yang, S. W.; Vosch, T. *ACS Nano* **2012**, *6*, 8803.
(31) Petty, J. T.; Fan, C.; Story, S. P.; Sengupta, B.; Sartin, M.; Hsiang, J. C.; Perry, J. W.; Dickson, R. M. *J Phys Chem B* **2011**, *115*, 7996.
(32) Huang, Z.; Tao, Y.; Pu, F.; Ren, J.; Qu, X. *Chemistry* **2012**, *18*, 6663.
(33) Cui, Q.; Shao, Y.; Ma, K.; Xu, S.; Wu, F.; Liu, G. *Analyst* **2012**, *137*, 2362.
(34) Zhang, P.; Wang, Y.; Chang, Y.; Xiong, Z. H.; Huang, C. Z. *Biosens Bioelectron* **2013**, *49*, 433.
(35) Zhang, M.; Guo, S. M.; Li, Y. R.; Zuo, P.; Ye, B. C. *Chem Commun (Camb)* **2012**, *48*, 5488.
(36) Zhao, T.-T.; Chen, Q.-Y.; Zeng, C.; Lan, Y.-Q.; Cai, J.-G.; Liu, J.; Gao, J. *Journal of Materials Chemistry B* **2013**, *1*, 4678.
(37) Feng, L.; Huang, Z.; Ren, J.; Qu, X. *Nucleic Acids Res* **2012**, *40*, e122.
(38) Schultz, D.; Gwinn, E. *Chem Commun (Camb)* **2011**, *47*, 4715.